Received: 12 September 2022 | Revised: 20 March 2023 | Accepted: 22 March 2023

https://doi.org/10.1016/j.jtha.2023.03.027

ORIGINAL ARTICLE

von Willebrand factor binds to angiopoietin-2 within endothelial cells and after release from Weibel–Palade bodies

Golzar Mobayen[1,*] | Koval Smith[2,*] | Kushani Ediriwickrema[1] | Richard D. Starke[2] | Emmanouil Georgios Solomonidis[1] | Michael A. Laffan[1] | Anna M. Randi[2] | Thomas A. J. McKinnon[1]

[1]Department of Immunology and Inflammation, Centre for Haematology, Imperial College London, Hammersmith Hospital Campus, London, United Kingdom

[2]National Heart and Lung Institute (NHLI) Cardiovascular Sciences, Unit Imperial College Academic Health Science Centre, Hammersmith Hospital, London, United Kingdom

Correspondence
Thomas A. J. McKinnon, Department of Immunology and Inflammation, Centre for Haematology, Imperial College London, 5th Floor, Commonwealth Building, Hammersmith Hospital Campus, Du Cane Road, London W12 0NN, United Kingdom.
Email: t.mckinnon03@imperial.ac.uk

Funding Information
T.A.J.M. was supported by a British Heart Foundation Intermediate Basic Science Fellowship grant (FS/11/3/28632) and R.D.S. by a British Heart Foundation Intermediate Basic Science Fellowship grant (FS/10/047/28393).

Abstract

Background: The von Willebrand factor (VWF) is a multimeric plasma glycoprotein essential for hemostasis, inflammation, and angiogenesis. The majority of VWF is synthesized by endothelial cells (ECs) and stored in Weibel–Palade bodies (WPB). Among the range of proteins shown to co-localize to WPB is angiopoietin-2 (Angpt-2), a ligand of the receptor tyrosine kinase Tie-2. We have previously shown that VWF itself regulates angiogenesis, raising the hypothesis that some of the angiogenic activity of VWF may be mediated by its interaction with Angpt-2.

Methods: Static-binding assays were used to probe the interaction between Angpt-2 and VWF. Binding in media from cultured human umbilical vein ECs s and in plasma was determined by immunoprecipitation experiments. Immunofluorescence was used to detect the presence of Angpt-2 on VWF strings, and flow assays were used to investigate the effect on VWF function.

Results: Static-binding assays revealed that Angpt-2 bound to VWF with high affinity ($K_{D,app}$ ~3 nM) in a pH and calcium-dependent manner. The interaction was localized to the VWF A1 domain. Co-immunoprecipitation experiments demonstrated that the complex persisted following stimulated secretion from ECs and was present in plasma. Angpt-2 was also visible on VWF strings on stimulated ECs. The VWF–Angpt-2 complex did not inhibit the binding of Angpt-2 to Tie-2 and did not significantly interfere with VWF-platelet capture.

Conclusions: Together, these data demonstrate a direct binding interaction between Angpt-2 and VWF that persists after secretion. VWF may act to localize Angpt-2; further work is required to establish the functional consequences of this interaction.

KEYWORDS
angiogenesis, angiopoietin-2, endothelial cells, von Willebrand factor, Weibel–Palade bodies

Manuscript handled by: David Lillicrap

Final decision: David Lillicrap, 23 March 2023

[*]Golzar Mobayen and Koval Smith contributed equally to this study.

1 | INTRODUCTION

The von Willebrand factor (VWF) is a large multimeric plasma glycoprotein that performs 2 roles essential to normal hemostasis; first, acting as the carrier molecule for procoagulant Factor VIII (FVIII) and second, supporting platelet adhesion at the sites of vascular injury [1,2]. The majority of plasma VWF is synthesized by endothelial cells (ECs) and is stored in Weibel–Palade bodies (WPB), which are released constitutively or available for release in response to endothelial stimulation [3]. Although the formation of WPB within EC is dependent on the presence of VWF, numerous other proteins have been shown to co-localize to WPB, including P-selectin, angiopoietin-2 (Angpt-2), FVIII, interleukin 8 (IL-8), eotaxin-3, endothelin, CD63, α1,3-fucosyltransferase VI, tissue-type plasminogen activator, osteoprotegerin (OPG), and IGFBP-7 and in some cases this is dependent on a binding interaction with VWF [4–14]. Indeed a number of recent studies have shown that several of the proteins targeted to WPB, namely, IL-8, P-selectin, and OPG, bind to VWF under the low pH and high calcium conditions understood to prevail in the Golgi apparatus [5,15,16]. Because the binding between VWF and other WPB constituents may persist after VWF exocytosis, this interaction may have important functional implications beyond co-localization and co-release [5,16,17].

This relationship is of particular relevance to Angpt-2 because *in vitro* and *in vivo* evidence has demonstrated that VWF regulates angiogenesis [18,19]. *In vitro*, inhibition of VWF expression by siRNA in human umbilical vein ECs (HUVECs) enhanced angiogenesis and increased vascular endothelial growth factor (VEGF)-dependent migration and proliferation of ECs, and enhanced Matrigel tube formation. *In vivo*, multiple studies have shown increased vascularization in VWF-deficient mice, both in baseline conditions such as the skin of the ear [18], and in response to ischemia in the brain [20]. Lack of VWF expression in HUVECs resulted in an increase in Angpt-2 levels in the culture media [18], suggesting that normal VWF expression has a role in targeting Angpt-2 to storage within EC and regulating its release. It is therefore important to understand the nature of the VWF–Angpt-2 interaction and its implications for Angpt-2 and VWF function.

Angpt-2 is a ligand for the endothelial tyrosine kinase receptor Tie-2 for which it competes with its counterpart Angpt-1 [21]. Initially, it was understood that binding of Ang1 to Tie-2 maintained a quiescent endothelium and that Angpt-2 acted as an antagonist of Tie-2 [22], but recent studies suggest that the action of Angpt-2 is contextual, promoting angiogenesis in the presence of VEGF but inducing vessel regression in its absence [23]. Binding to VWF may provide an additional important context for Angpt-2 function by localizing it to the endothelial surface and modulating its interaction with Tie2.

We now report that Angpt-2 is able to bind to VWF in a calcium- and pH-dependent manner, consistent with binding in the Golgi, and that this interaction is maintained at physiological pH following WPB exocytosis and persists in plasma. Furthermore, we demonstrate that binding of Angpt-2 to VWF does not alter its ability to bind to Tie-2 nor does it significantly affect the platelet capture potential of VWF.

Essentials

- von Willebrand factor stored in Weibel–Palade bodies (WPBs) mediates angiogenesis.
- A range of proteins including angiopoietin-2 (Angpt-2) are also stored in WPBs.
- Angpt-2 binds with high affinity to the VWF A1 domain and remains complexed to VWF upon endothelial secretion.
- Angpt-2 binding to VWF has no impact on the VWF-platelet capture function.

2 | MATERIALS AND METHODS

2.1 | Expression and purification of proteins

Recombinant Angpt-2 and Tie-2–Fc were purchased from R&D Systems. Plasma-derived (pd) VWF was purified by gel filtration chromatography from Haemate P as previously described [24]. Full-length (FL) recombinant *VWF*, deletion (Δ) A1 and A3 variants, and a panel of VWD type 2B, 2M and 2A variants were generated using site-directed mutagenesis and expressed in HEK293T. A *VWF* composite variant containing 6 mutations in the A1 domain heparin-binding region (Arg1334Ala, Lys1335Ala, Arg1336Ala, Arg1341Ala, Arg1342Ala, and Lys1348Ala) termed VWF-6A was generated using sequential mutagenesis and also expressed in HEK293T cells. *VWF* variants: A1 (residues 1238-1493), A2 (1498-1671), A1CK (residues 1260-2813), A2CK (1472-2813), and A3CK (1671-2813), were constructed using standard molecular biology techniques in the mammalian expression vector pcDNA3.1 and expressed in HEK293T cells and purified by Nickel affinity chromatography.

2.2 | Static-binding assays

Maxisorp plates (Nunc) were coated with pdVWF at a final concentration of 20 μg/mL in carbonate buffer (pH 9.6) overnight at 4°C. Wells were washed 3 times in phosphate-buffered saline supplemented with 0.1% Tween-20 (phosphate-buffered saline [PBS-T]) and then blocked with 2% bovine serum albumin (BSA). To determine the effect of pH and calcium on the interaction, Angpt-2 was diluted to a final concentration of 10 nM in 20 mM Bis–Tris with varying pH (5–7.4) and $CaCl_2$ (0–100 mM) for 60 minutes at room temperature. Bound Angpt-2 was detected with biotinylated anti-Angpt-2 (R&D systems) followed by streptavidin–horse radish peroxidase (HRP).

SIGMAFAST OPD was added to the wells and the reaction stopped with 2 M H_2SO_4 and the absorbance was recorded at 492 nm. All subsequent binding assays were performed in Bis–Tris pH 6.5 with 10 mM $CaCl_2$. To derive the $K_{D,app}$ for the interaction, VWF-coated wells were incubated with increasing concentrations of Angpt-2 and fitted to the one-site binding equation using Prism Software for Science software package (Version 7.0; GraphPad Software). In reciprocal assays, Maxisorp plates were coated with 50 nM Angpt-2 and following washing and blocking, incubated with increasing concentrations of VWF. Bound VWF was detected with polyclonal anti-VWF-HRP (Dako). To establish the region of VWF responsible for the interaction, Angpt-2-coated wells were incubated with 30 nM of each VWF construct. Bound VWF was detected with rabbit anti-VWF (Santa Cruz) directed against C-terminal residues 2514-2813, and goat antirabbit-HRP secondary antibody (Dako). All wash and antibody incubation steps were performed using PBS-T pH 7.4. No effect of performing washing or antibody steps using 20 mM Bis–Tris, Tween-20 0.1% (v/v) was observed (data not shown).

2.3 | Co-immunoprecipitation of VWF and Angpt-2 from HUVEC culture media and plasma

HUVECs were cultured as previously described in 6 well plates and where stated stimulated with tumor necrosis factor-alpha (TNFα; Sigma) for 4 hours and 100 μM histamine for 15 min. Plasma samples were obtained from healthy volunteers not taking any medication. For immunoprecipitation, 1.5 mL of HUVEC media or plasma were precleared with EZview protein G agarose (Sigma) overnight at 4°C. The precleared samples were then immunoprecipitated with Tosyl-activated M-280 Dynabeads or Protein G Dynabeads, coupled to polyclonal anti-VWF, anti-Angpt-2, or irrelevant IgG antibodies according to manufacturer's instructions, for 3 hours at room temperature. Beads were washed 5 times with PBS-T and bound proteins eluted with 2 × LDS buffer (Invitrogen) supplemented with 3% (v/v) beta-mercaptoethanol and heating at 90°C for 15 min. Eluted proteins were run through 4%–12% SDS-PAGE gels (Invitrogen), followed by Western blotting and probing with specific antibodies. To determine the proportion of plasma Angpt-2 bound to plasma VWF, plasma Angpt-2 was analyzed by Angpt-2 ELISA (R&D systems) before and after immunoprecipitation with anti-VWF antibodies.

2.4 | Tie-2 binding assay

pdVWF (10 μg/mL) was incubated with 10 nM Angpt-2 in 20 mM Bis–Tris, 10 mM $CaCl_2$, pH 6.5 for 60 minutes at room temperature in a final volume of 500 μL. 1 M Tris pH 9.0 was then added to raise the pH to 7.4; and 100 ng recombinant Tie-2-Fc (R&D Systems) was added to the reaction and incubated for a further 60 minutes at room temperature. Complexes were immunoprecipitated by the addition of 50 μL Protein G Dynabeads (Invitrogen) for 15 min, followed by 3 washes with PBS-T. Proteins were eluted and analyzed as described.

2.5 | Immunofluorescence microscopy

To visualize Angpt-2 on VWF strings, HUVECs were treated with 10 ng/mL Angpt-2 for 4 hours and then stimulated with 100 μM histamine for 5 min, prior to fixation and staining. Immunofluorescence microscopy was performed as described previously [18].

2.6 | siRNA knock down of Angpt-2 in HUVECs

HUVECs were obtained from Lonza and cultured in endothelial growth media-2 as previously described [18]. Cells were used between passages 2–4. For siRNA knock down, cells were seeded in 6 well plates until 70% confluent and then transfected with either AllStars-negative control scrambled siRNA (Qiagen) or siRNA directed against Angpt-2 (Santa Cruz) at a final concentration of 10 nM using lipofectamine 3000 (Invitrogen).

To examine the effect of Angpt-2 knock down on platelet capture; 24 hours post transfection, cells were washed and detached and seeded into Ibid $VI^{0.4}$ channel slides and the remainder into the wells of a 12-well plate. Twenty-four hours post seeding, the cells were treated with 10 ng/mL TNFα for 4 h, then cells in Ibidi $VI^{0.4}$ (Ibidi) slides were further stimulated with 100 μM histamine for 3 minutes to induce VWF release and perfused with washed platelets and red blood cells containing $DiOC_6$ to render platelets fluorescent. Platelet binding to VWF strings was visualized in real time and analyzed off-line using ImageJ software. In addition, the cells from the 12-well plate were detached and pelleted, and then lysed with 100 μL RIPA buffer. Equal amounts (10 μg) were electrophoresed through 4%–12% SDS-PAGE gels and then Western blotted onto nitrocellulose membranes, and membranes were blocked with 5% powdered milk in 0.1% PBS-Tween. Angpt-2 was detected with polyclonal goat anti-Angpt-2 antibodies (R&D systems) at 1 μg/mL and rabbit anti-goat-HRP antibodies. β-actin was detected using mouse anti-β-actin antibodies and anti-mouse-HRP.

2.7 | Platelet adhesion to VWF–Angpt-2 complexes under shear stress

Ibidi $VI^{0.1}$ flow chamber slides were coated with pdVWF at a final concentration of 30 μg/mL overnight in carbonate buffer. Following washing and blocking with 2% BSA, some channels were incubated with 10 nM Angpt-2 in 10 mM Bis–Tris, 10 mM $CaCl_2$, pH 6.5 for 60 min. Binding of Angpt-2 to VWF in these channels was confirmed by the addition of biotinlayted anti-Angpt-2 and the subsequent addition of streptavidin–HRP and OPD substrate (data not shown). Washed platelets labeled with 10 μM DiOC6 and washed red blood cells prepared as previously described were perfused through the channels at 1000/s and the real-time movies captured after 5 minutes of flow and the number of platelets captured and the translocation velocity of platelets over 20-second periods were analyzed off-line using ImageJ software as previously described [25].

2.8 | Statistical analysis

Data analysis was performed using the Prism Software. Results are expressed as means ± SEM. The statistical significance of differences between the 2 groups was assessed using one-way analysis of variance.

3 | RESULTS

3.1 | Angpt-2 binds to VWF in a calcium- and pH-dependent manner

We first examined the interaction of Angpt-2 with VWF using plate-binding assays over a pH range from 5 to 7.4. Angpt-2 (10 nM) bound to immobilized VWF in a pH-dependent manner, with binding increasing up to a maximum at pH 6.5 and then decreasing as the pH was raised further (Figure 1A). We then investigated binding in the presence of increasing calcium concentrations from 0 to 60 mM and observed maximal binding at 10 mM calcium (Figure 1B). Similar to the previously published data for the interaction of OPG with VWF [16], these data are consistent with Angpt-2 interacting with VWF in the Golgi body, where the pH is acidic and the calcium concentration is elevated.

3.2 | Angpt-2 binds predominantly to the VWF A1 domain with high affinity

Using the determined optimal binding conditions, plate-bound VWF was incubated with increasing concentrations of Angpt-2 at pH 6.5 with 10 mM $CaCl_2$. Angpt-2 bound to VWF with high affinity; $K_{D,app}$ = 5.1 ±0.4 nM (Figure 2A). When binding assays were repeated with Angpt-2-coated wells and VWF in solution, a similar $K_{D,app}$ was derived: 3.1 nM ± 0.2 nM (Figure 2B), indicating that VWF conformation does not influence the interaction. To establish the region of VWF involved in the interaction, microtiter plates were coated with Angpt-2 and incubated with a panel of *VWF* variants. The ΔA3 and A1-CK constructs bound to Angpt-2 in a comparable fashion to both plasma purified and recombinant FL VWF (Figure 2C). However, the ΔA1, A2-CK, A3-CK constructs showed significantly reduced binding (Figure 2C). Moreover, binding occurred between the isolated VWF A1 domain and Angpt-2, but no binding was observed to the isolated VWF A2 domain (Figure 2D). Together, these data demonstrate that Angpt-2 binds predominantly to the VWF A1 domain.

3.3 | Mutations in the VWF A1 domain but not the A2 domain have decreased Angpt-2 binding

To further investigate the binding of Angpt-2 to VWF, a panel of recombinant VWF proteins with known type 2B, 2M, and 2A VWD-causing mutations were generated and screened for binding to Angpt-2. Interestingly, the majority of the type 2M (red bars) and 2B variants (blue bars) tested had significantly reduced binding to Angpt-2 (Figure 3Ai). The Pro1467Ser variant, which affects the ristocetin-binding site but not VWF function [26], did not affect Angpt-2 binding. Additionally, the VWF-6A variant, which contains 6 mutations in the heparin-binding region of VWF located in the A1 domain, did not alter Angpt-2 binding to VWF (Figure 3Aii). In contrast, the type 2A variants, except for the Ser1613Pro variant, all had similar or in some cases significantly enhanced binding to Angpt-2 (Figure 3B). These data are consistent with the Angpt-2-binding site being located within the VWF A1 domain but distinct from the heparin-binding site. Mapping the panel of type 2M and 2B variants onto the crystal structure of the A1 domain, however, did not reveal a distinct binding site, suggesting that mutations in the A1 domain disrupt the overall structure, leading to defective Angpt-2 binding (Figure 3C).

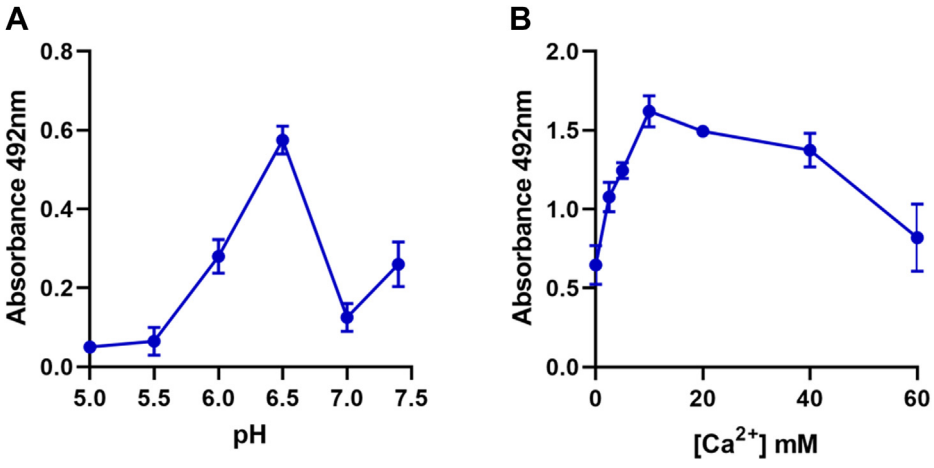

FIGURE 1 Angpt-2 binds to VWF in a pH and calcium-dependent manner. Immobilized VWF was incubated with 10 nM Angpt-2 at different pH (A) and increasing $CaCl_2$ concentrations (B). Bound Angpt-2 was detected with biotinylated mouse anti-Angpt-2 and streptavidin–HRP conjugated antibodies. (Error bars represent mean ± SEM of 3 experiments performed in duplicate). HRP, horse radish peroxidase; VWF, von Willebrand factor.

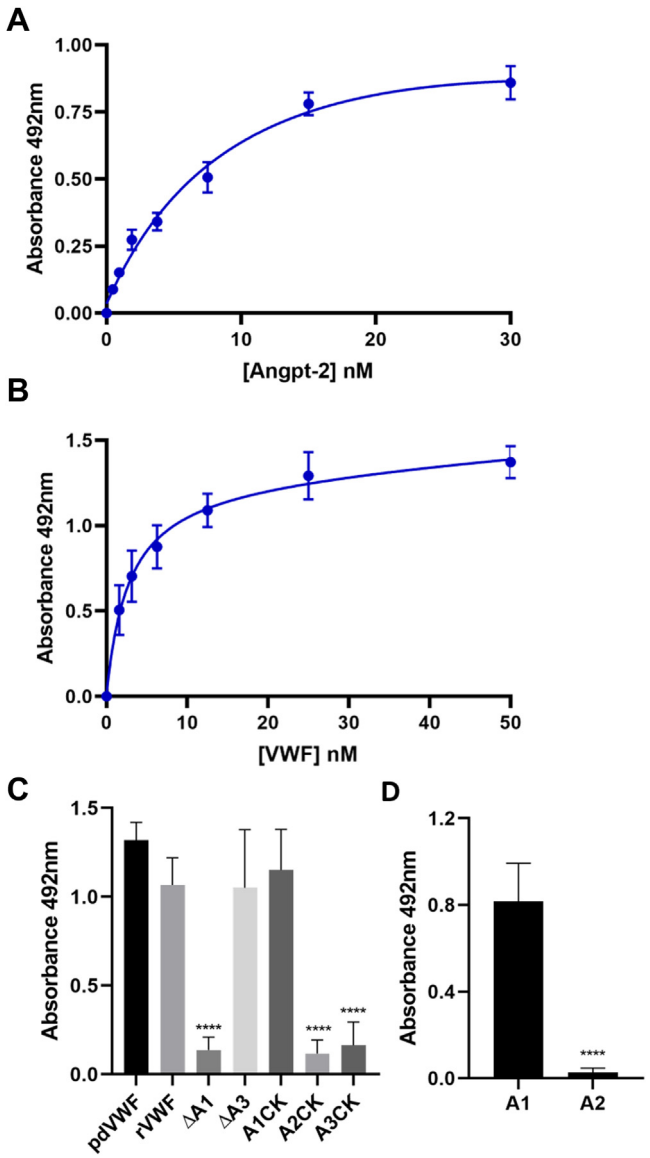

FIGURE 2 Angpt-2 binds to the VWF A1 domain, and binding is not dependent on VWF conformation. (A) Immobilized VWF (20 μg/ml) was incubated with increasing concentrations of Angpt-2 in 20 mM Bis–Tris pH 6.5/10 mM $CaCl_2$. Bound Angpt-2 was detected with biotinylated mouse anti-Angpt-2 and streptavidin–HRP conjugated antibodies. (B) Immobilized Angpt-2 (50 nM) was incubated with increasing concentrations of purified plasma-derived VWF in 20 mM Bis–Tris pH 6.5/10 mM $CaCl_2$ and bound VWF detected with anti-VWF–HRP antibodies. Both binding curves were fitted using Prism Software for Sciene (Version 7.0; GraphPad Software) using the 1-site binding equation. (C) VWF constructs at 30 nM final concentration were incubated with immobilized Angpt-2 and detected with rabbit anti-VWF–C-terminal antibodies and antirabbit-HRP conjugated secondary antibody. (D) Recombinant VWF A1 or A2 domain was incubated with immobilized Angpt-2 and detected with anti–Myc-Tag-HRP antibodies. (Error bars represent mean ± SEM of 3 experiments performed in duplicate). HRP, horse radish peroxidase; VWF, von Willebrand factor.

3.4 | The VWF–Angpt-2 complex is maintained following release from ECs and is present in plasma

We then investigated whether the VWF–Angpt-2 interaction was maintained following secretion from WPBs. HUVECs were treated with 10 ng/mL TNFα for 4 hours to upregulate Angpt-2 expression [27], and then stimulated with 100 μM histamine for 15 minutes to induce WPB exocytosis. Immunoprecipitates from the cell culture medium using polyclonal anti-Angpt-2 or anti-VWF antibodies were analyzed by SDS-PAGE followed by Western blotting with anti-VWF–HRP. Following TNFα treatment and histamine stimulation, a significant amount of VWF was co-immunoprecipitated with Angpt-2, providing further evidence that Angpt-2 binding to VWF occurs within the cell, persists in the WPB and is maintained following exocytosis (Figure 4A). It has been previously shown that OPG and VWF remain complexed in plasma; therefore, we determined whether the same is true of VWF and Angpt-2. VWF and Angpt-2 could be reciprocally immunoprecipitated from human plasma (Figure 4B). To investigate the relationship between free and VWF–Angpt-2, we determined the plasma levels of Angpt-2 before and after immunoprecipitation with anti-VWF antibodies. In all plasma samples, the concentration of Angpt-2 decreased after immunoprecipitation of VWF with an average decrease of 68.3%, indicating that ~30% of circulating Angpt-2 is unbound to VWF (Figure 4C). To explore the relationship between VWF and Angpt-2 release from cultured ECs, we performed confocal microscopy on TNFα-treated HUVECs activated with histamine to stimulate the release of VWF. IF staining showed co-localization of Angpt-2 on VWF strings released from activated ECs (Figure 4D). Together, these data show that Angpt-2 can remain in a complex with VWF following release from ECs.

3.5 | Angpt-2 in a complex with VWF is able to bind to Tie-2

Because the interaction between VWF and Angpt-2 persists following secretion, we investigated its effect on Angpt-2 binding to its receptor on the EC surface, Tie2. The VWF–Angpt-2 complex was formed at pH 6.5, following which the pH was raised to 7.4. The complex was then incubated with recombinant Tie-2–Fc. As a control, Angpt-2 or VWF alone were also incubated with Tie-2–Fc. Tie-2–Fc was immunoprecipitated with protein G Dynabeads, and the immunoprecipitates were analyzed by SDS-PAGE followed by Western blotting with antibodies specific for VWF, Angpt-2, and Tie-2. As expected, Angpt-2 alone was able to bind and co-immunoprecipitate with Tie-2, whereas VWF alone was not. However, when the Angpt-2–VWF complex was incubated with Tie-2, VWF was co-immunoprecipitated, indicating that Angpt-2 can bind simultaneously to both molecules (Figure 5A). Similarly, when Angpt-2 was complexed with VWF and incubated with immobilized Tie-2–Fc, binding to VWF did not affect the ability of Angpt-2 to interact with Tie-2 (Figure 5B).

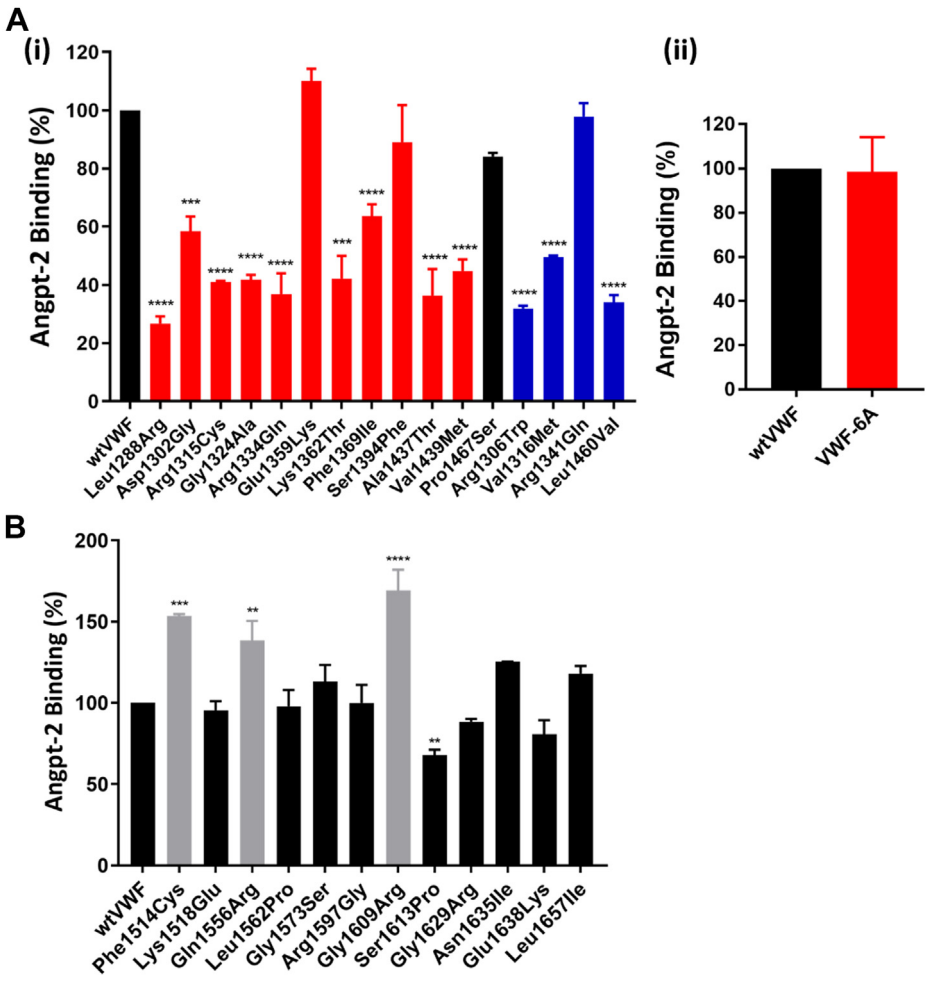

FIGURE 3 Binding of type 2B and 2M VWD variants located in the A1 domain of VWF have reduced binding to Angpt-2. Maxisorp plates coated with Angpt-2 were incubated 10 μg/mL wild-type recombinant VWF or a panel of type 2B, 2M, and 2A von Willebrand disease causing variants in 20 mM Bis–Tris pH 6.5/10 mM $CaCl_2$ and bound VWF detected with anti-VWF–HRP antibodies. (Ai) Interaction of type 2M (red bars) and 2B (blue bars) with immobilized Angpt-2. Pro1467Ser variant is shown in black. (Aii) Interaction of VWF-6A with immobilized Angpt-2. (B) Interaction of type 2A variants with Angpt-2. Black bars represent variants with normal binding compared with wtVWF, gray bars represent variants with increased Ang2 binding. (C) Mapping of the VWD variants on the crystal structure of the VWF A1 domain using Pymol (protein database code 1AUQ). HRP, horse radish peroxidase; VWF, von Willebrand factor.

3.6 | Binding of Angpt-2 to the VWF A1 domain does not alter the platelet capture function

Given the observation that Angpt-2 binds to the VWF A1 domain and remains bound following secretion from the endothelium, we speculated that this may affect the interaction of the VWF A1 domain with GPIbα. To investigate this, we first examined VWF-platelet string formation on HUVECs treated with siRNA against Angpt-2. Despite a slight trend toward less platelet capture on Angpt-2 knock down cells, no significant difference in platelet string formation was seen in the absence of Angpt-2 (Figure 6A, B). Next, we coated Ibidi $VI^{0.4}$ flow slides with 30 μg/mL VWF then bound Angpt-2 (20 nM) at pH 6.5/10 mM $CaCl_2$ and perfused over platelets and red blood cells at 1000/s. No significant difference was seen between the extent of platelet capture by VWF complexed with or without Angpt-2 (Figure 6D, E).

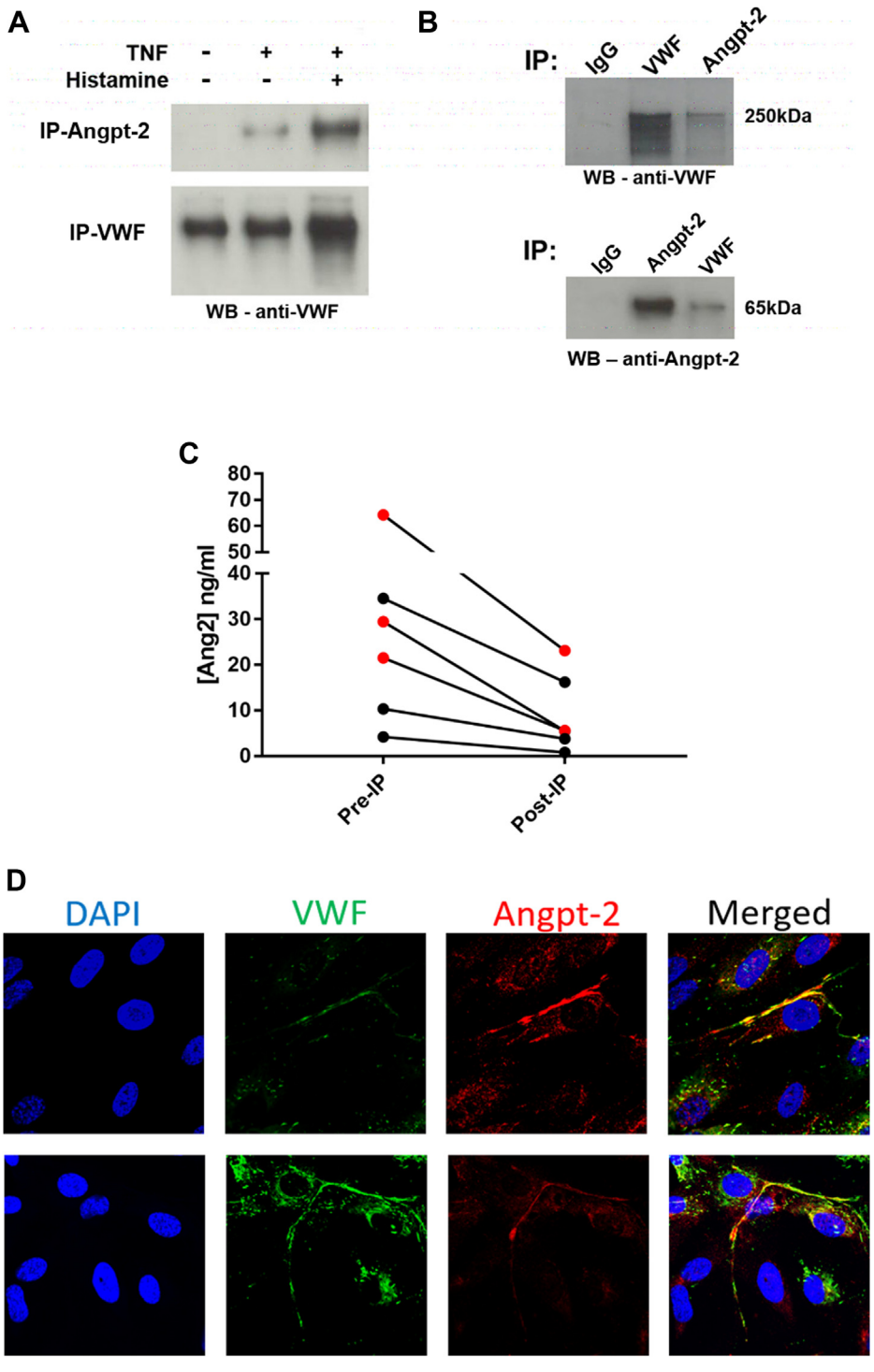

FIGURE 4 The VWF–Angpt-2 complex is maintained following secretion from HUVECs and is present in plasma. (A) HUVECs cultured in EBM-2 were seeded onto 6-wells plates and allowed to reach confluency. Cells were treated with 10 ng/mL TNFα for 4 hours and then stimulated with 100 μM histamine for 3 minutes. Media was immunoprecipitated with protein G Dynabeads coupled to either polyclonal anti-VWF or anti-Angpt-2 antibodies. Proteins were released from the beads by heating at 95°C with 2×SDS gel loading buffer with 3% β-mercaptoethanol, then electrophoresed through 4%–12% gels. Then, Western blotting membranes were probed with anti-VWF–HRP antibodies. (B) Pooled plasma from 4 donors was precleared overnight with protein G agarose beads, then immunoprecipitated with M-280 Tosylactivated beads coupled to either anti-VWF or anti-Angpt-2 antibodies or control IgG. Bound proteins were eluted by heating at 70°C in 2× SDS gel loading buffer with 3% β-mercaptoethanol. (C) Plasma samples from 3 healthy controls (black circles) and 3 patients with COVID-19 (red circles) were immunoprecipitated with polyclonal anti-VWF antibodies. Plasma Angpt-2 levels before and after immunoprecipitation were measured using an Angpt-2 ELISA. (D) HUVECs were stimulated with histamine, and VWF strings released onto the cell surface were stained with antibodies specific to VWF and Angpt-2 and appropriate secondary antibodies conjugated with fluorescent dyes. Images were taken at ×63 zoom on a Leica Stellaris 8 confocal. Representative images are shown from 2 separate experiments. Angpt-2, angiopoietin-2; HRP, horse radish peroxidase; HUVEC, human umbilical vein endothelial cell; VWF, von Willebrand factor.

4 | DISCUSSION

The synthesis of VWF in ECs drives the formation of WPBs that, together with VWF, store a range of proteins involved in hemostatic, inflammatory, and angiogenic pathways. The mechanism by which co-storage of proteins with VWF is achieved seems to be variable. For example, P-selectin can bind to VWF, but its storage in WPB is independent of this interaction [5], although FVIII binds closely to VWF in plasma, binding to intracellular VWF is not necessary for FVIII storage in WPB [28]. Nonetheless, a number of studies have demonstrated that binding to VWF targets several proteins for WPB storage. Our previous studies indicated that in the absence of VWF, Angpt-2

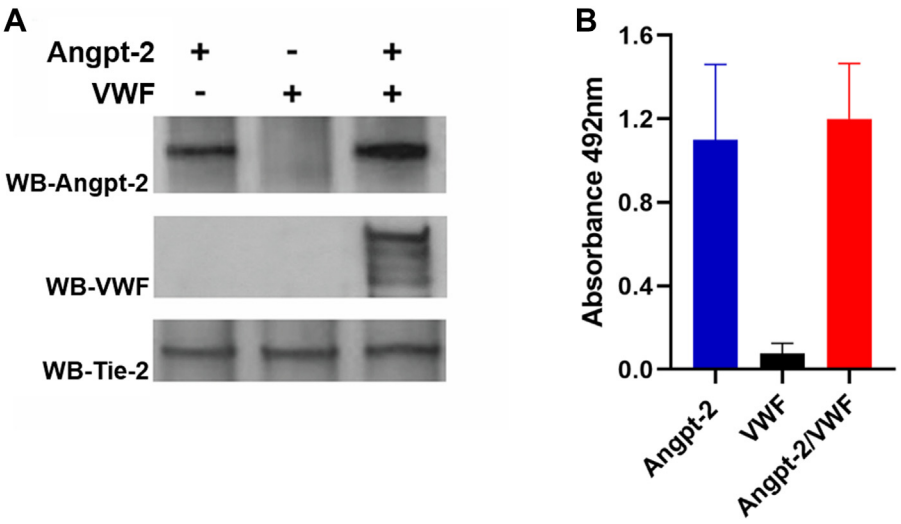

FIGURE 5 Angpt-2 complexed to VWF can bind to Tie-2. (A) Angpt-2 was incubated with and without VWF at pH 6.5/10 mM $CaCl_2$ and then the pH raised to 7.4. Samples were then incubated with soluble Tie-2–Fc and immunoprecipitated with Protein G and run on SDS-PAGE gels followed by Western blotting and probing with either anti-Angpt-2, anti-VWF, or anti-Tie-2 antibodies. (B) Angpt-2 and VWF were complexed as above and incubated with immobilized Tie-2–Fc. Bound Angpt-2 was detected with mouse anti-Angpt-2 and antimouse-HRP antibodies. Angpt-2, angiopoietin-2; HRP, horse radish peroxidase; VWF, von Willebrand factor.

release from EC is increased, consistent with regulated release being dependent on VWF and WPB formation [18]. In addition, VWD patients can experience gastrointestinal bleeding linked to angiodysplasia, and this is more frequent in patients with type 2A or very low VWF plasma level [29–31]. We have previously proposed that VWF may control angiogenesis partly by regulating Angpt-2 storage and that abnormal angiogenesis may be responsible for angiodysplasia seen in some patients with VWF deficiency (VWD) [32]. Similarly, Selvam et al. [33] demonstrated that endothelial colony-forming cells from patients with type 1 and type 3 VWD exhibited increased Angpt-2 secretion, consistent with the lack of organelle storage. In the present study, we have identified that Angpt-2 interacts with VWF with high affinity, which helps explain these previous findings. In static phase binding assays, Angpt-2 bound to VWF at pH 6.5 in the presence of 10 mM $CaCl_2$, consistent with conditions thought to prevail in the Golgi body [34–36] and which have been previously reported to be optimal for VWF binding to other WPB components, OPG and IL-8 [15,16]. It remains to be established whether binding occurs following multimerization or during the formation of VWF multimers. However, plate-bound VWF and globular VWF had similar affinities for Angpt-2; this would suggest that a conformational change is not required for the interaction to occur. Interestingly, we found that Angpt-2 binds predominantly to the A1 domain of VWF. This is also supported by our observations that causative VWD mutations in the A1 but not in the A2 domain reduced binding to Angpt-2. Although the spectrum of A1 domain variants tested did not localize the Angpt-2 binding site, it is likely that mutations in the A1 domain disrupt the domain structure to the extent that Angpt-2 binding is reduced. We have recently shown that the heparin-binding domain present in the A1 domain of VWF promotes the binding of multiple growth factors to VWF, including VEGF-A and fibroblast growth factor-2 [37]. Interestingly, the VWF-6A variant that contains 6 point mutations in the heparin-binding site and causes >60% reduction in heparin binding did not exhibit reduced binding to Angpt-2 [38]. Moreover, the Arg1341Gln variant, that in our previous study reduced binding to VEGF-A, did not affect Angpt-2 binding. Together these data suggest that the residues involved in VWF-binding Angpt-2 are distinct from the heparin-binding site. The finding that type 2B and 2M VWD mutations cause reduced Angpt-2 binding raises the conjecture that patients with mutations in the A1 domain may have altered Angpt-2 storage; however, Groeneveld et al. [39] observed plasma concentrations of Angpt-2 and OPG in 654 VWD patients and found no significant differences in the concentrations of either proteins between the 3 main VWD types. Although they observed higher plasma Angpt-2 concentrations in type 2B patients, there was no statistical significance. However, in the same study, mutations linked to increased clearance and reduced VWF synthesis resulted in increased Angpt-2 levels. It is worth noting, however, that plasma Angpt-2 levels are generally low in the healthy state and are only increased following vascular perturbation. Further mapping studies will be required to fully define which residues are crucial for binding and whether VWD mutations in the A1 domain can affect Angpt-2 storage.

Significantly, the VWF–Angpt-2 complex remained intact following secretion from ECs and similar to data shown for OPG, Angpt-2 could be localized to VWF strings following stimulated release from HUVECs; and complexes of Angpt-2 with VWF were also present in human plasma, indicating that *in vivo* the interaction persists following the release of VWF from ECs. This indicates that despite the change in acidic pH from the WPB to the near neutral pH of either cell media or plasma, the interaction is effectively maintained. Supporting this, studies on the role of VWF targeting FVIII to WPBs have shown that FVIII is able to bind to VWF in a pH range of 6.2–7.4 with a reduction in binding affinity only seen at pH 5.5 [40], indicating that FVIII can bind with high affinity to VWF at low pH and remains associated following secretion. To determine the proportion of Angpt-2 bound to VWF in plasma, we measured plasma Angpt-2 levels before and after immunoprecipitation of VWF. In all samples a reduction in the Angpt-2 level was observed, with an average reduction of ~70%. This suggests that despite the high-affinity interaction of Angpt-2 with VWF, ~30% of plasma Angpt-2 is not

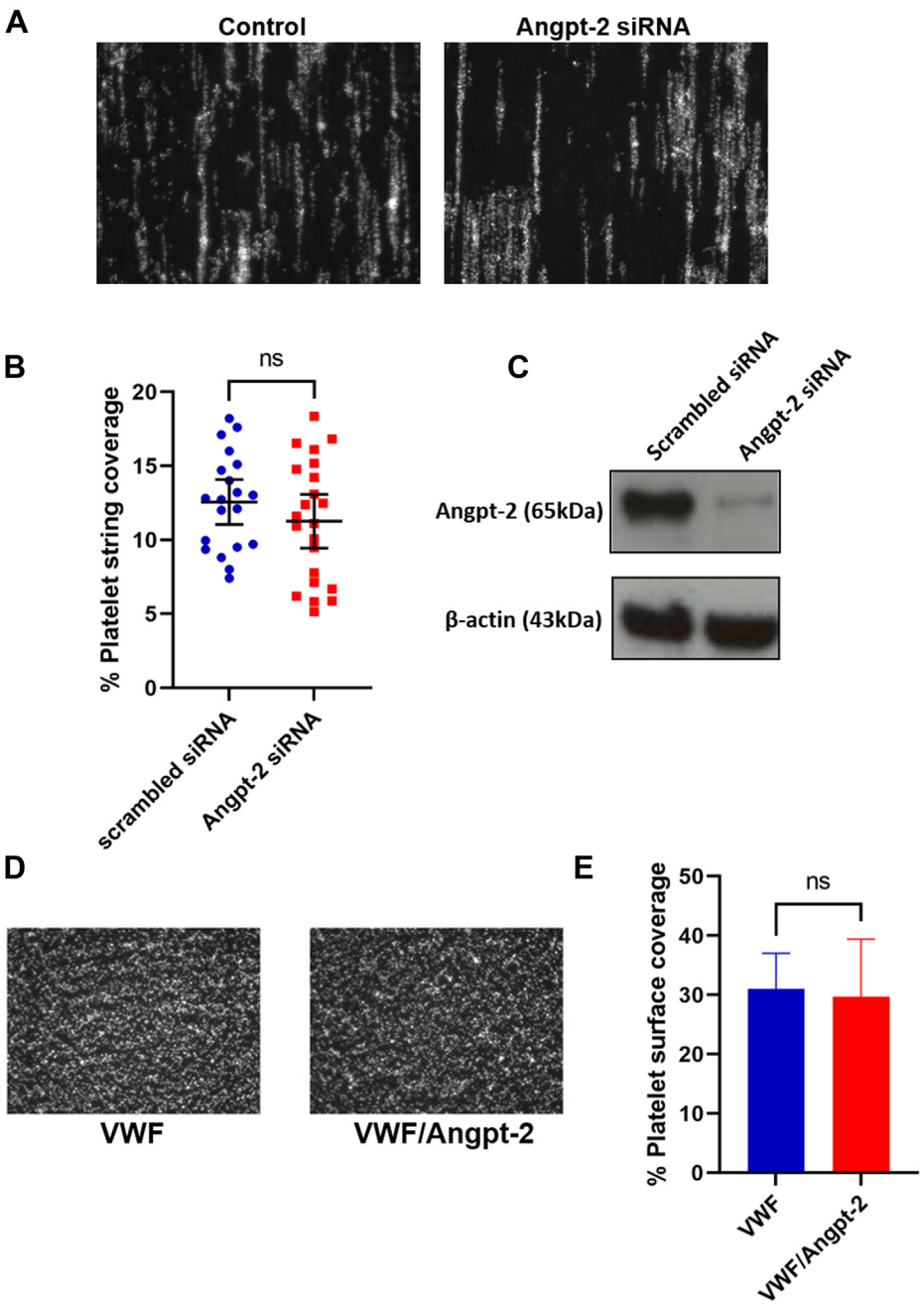

FIGURE 6 Effect of Angpt-2 on platelet capture to VWF. (A, B) HUVECs treated with scrambled siRNA (control) or siRNA against Angpt-2 were cultured in Ibidi VI$^{0.1}$ slides, stimulated with TNFα and histamine, and perfused with washed red blood cells and platelets for 3 minutes. Platelet string formation was visualized in real-time and platelet string coverage was determined using Image J software. (C) Western blot analysis of siRNA knock down of Angpt-2 in TNFα-treated cells. (D, E) Ibidi VI$^{0.1}$ flow slides were coated with 30 μg/mL purified VWF and then incubated with Angpt-2 diluted in 20 mM Bis–Tris, 10 mM $CaCl_2$, pH 6.5 for 1 hour. Slides were then perfused with washed red blood cells and platelets at 1000/s for 5 minutes. Images were captured after 5 minutes of perfusion and the platelet surface coverage was determined. Angpt-2, angiopoietin-2; HUVEC, human umbilical vein endothelial cell; TNFα, tumor necrosis factor-alpha; VWF, von Willebrand factor.

bound to VWF. Because VWF expression is not uniform in all vascular beds and Angpt-2 expression can occur in the absence of VWF, it can therefore be secreted without VWF and can circulate without the need to be in complex. Furthermore, because the complex appears to preferentially form under conditions present inside the Golgi, the plasma milieu may not represent the environment needed for the interaction and thus free-circulating Angpt-2 would fail to interact with circulating VWF.

The persistence of the majority of the VWF–Angpt-2 complex following secretion suggests that VWF may be able to modulate Angpt-2 function, potentially stabilizing and protecting Angpt-2 from clearance. It is interesting to note that the half-life of Angpt-2 is ~18 hours [6]. Although the half-life of VWF varies between individuals (4–26 hours) [41], it is conceivable that VWF may contribute to the long half-life of Angpt-2 by protecting it from clearance. Alternatively, the interaction may aid in localizing Angpt-2 to sites of inflammation or injury. Indeed, the VWF–Angpt-2 complex was still able to interact with Tie-2; therefore, the interaction with VWF may function to maintain a high local concentration of Angpt-2 following release from the endothelium in response to stimuli. Further to this, the elevation of VWF and Angpt-2 has been demonstrated in a number of disease states. For example, both VWF and Angpt-2 concentrations are significantly increased in severe sepsis and correlate with disease severity [42–44]. Likewise, EC activation in COVID-19 infection results in enhanced plasma VWF and Angpt-2, and their concentrations are associated with the severity of COVID-19 disease [45,46]. Thus, it

may be of clinical interest to determine the proportion of free and VWF complexed Angpt-2 within the plasma of patients. Of the 6 plasma samples used in this study, 3 were from COVID-19 patients who we had previously shown to have high plasma Angpt-2 levels [45]. We did not observe any differences between the ratio of bound and unbound Angpt-2 compared with the 3 control plasma samples; however, this is a highly limited sample number and further work is needed to explore this. We also investigated the effect of Angpt-2 complexed with VWF on the ability of VWF to capture platelets. Despite a trend to reduced platelet capture, no difference in the platelets string surface coverage was observed between control and Angpt-2–deficient cells. We also performed flow experiments where the VWF–Angpt-2 complex was formed on a flow channel, and platelet capture was examined in real time under shear stress. No numerical difference was observed in platelet capture in the presence or absence of Angpt-2, suggesting that Angpt-2 bound to VWF does not affect the ability of VWF to bind to GPIbα on the platelet surface. This is in contrast to recent data from Wohner et al. [47] that demonstrated reduced platelet binding to VWF in the presence of OPG, indicating distinct binding sites for OPG and Angpt-2 on VWF.

In conclusion, these data confirm that Angpt-2 is a novel binding partner for the A1 domain of VWF that does not appear to significantly influence VWF function. Further work is needed to establish the functional significance of the interaction, but it is likely that VWF mediates the storage of Angpt-2.

ACKNOWLEDGMENTS

T.A.J.M. was supported by a British Heart Foundation Intermediate Basic Science Fellowship grant (FS/11/3/28632) and R.D.S. by a British Heart Foundation Intermediate Basic Science Fellowship grant (FS/10/047/28393). We are grateful for support from the Imperial College BRC.

AUTHOR CONTRIBUTIONS

T.A.J.M. designed the study, performed experiments, analyzed the results, and wrote the manuscript; R.D.S. performed experiments, analyzed the results, and wrote the manuscript; K.E. and G.M. performed experiments. K.S. analyzed data. E.G.S. performed experiments. A.M.R. designed the study, analyzed the results, and wrote the manuscript; M.A.L. designed the study, analyzed the results and wrote the manuscript. All authors read and approved the final version of the paper.

DECLARATION OF COMPETING INTERESTS

The authors declare no competing financial interests.

REFERENCES

[1] Nogami K, Shima M, Nishiya K, Hosokawa K, Saenko EL, Sakurai Y, Shibata M, Suzuki H, Tanaka I, Yoshioka A. A novel mechanism of factor VIII protection by von Willebrand factor from activated protein C-catalyzed inactivation. *Blood*. 2002;99:3993–8.

[2] Sadler JE. Biochemistry and genetics of von Willebrand factor. *Annu Rev Biochem*. 1998;67:395–424.

[3] Wagner DD. Cell biology of von Willebrand factor. *Annu Rev Cell Biol*. 1990;6:217–46.

[4] Bonfanti R, Furie BC, Furie B, Wagner DD. PADGEM (GMP140) is a component of Weibel–Palade bodies of human endothelial cells. *Blood*. 1989;73:1109–12. PMID: 2467701.

[5] Michaux G, Pullen TJ, Haberichter SL, Cutler DF. P-selectin binds to the D′-D3 domains of von Willebrand factor in Weibel-Palade bodies. *Blood*. 2006;107:3922–4.

[6] Fiedler U, Scharpfenecker M, Koidl S, Hegen A, Grunow V, Schmidt JM, Kriz W, Thurston G, Augustin HG. The Tie-2 ligand angiopoietin-2 is stored in and rapidly released upon stimulation from endothelial cell Weibel–Palade bodies. *Blood*. 2004;103:4150–6.

[7] Romani de Wit T, de Leeuw HP, Rondaij MG, de Laaf RT, Sellink E, Brinkman HJ, Voorberg J, van Mourik JA. Von Willebrand factor targets IL-8 to Weibel-Palade bodies in an endothelial cell line. *Exp Cell Res*. 2003;286:67–74.

[8] Oynebraten I, Bakke O, Brandtzaeg P, Johansen FE, Haraldsen G. Rapid chemokine secretion from endothelial cells originates from 2 distinct compartments. *Blood*. 2004;104:314–20.

[9] Zannettino AC, Holding CA, Diamond P, Atkins GJ, Kostakis P, Farrugia A, Gamble J, To LB, Findlay DM, Haynes DR. Osteoprotegerin (OPG) is localized to the Weibel–Palade bodies of human vascular endothelial cells and is physically associated with von Willebrand factor. *J Cell Physiol*. 2005;204:714–23.

[10] Ozaka T, Doi Y, Kayashima K, Fujimoto S. Weibel-Palade bodies as a storage site of calcitonin gene-related peptide and endothelin-1 in blood vessels of the rat carotid body. *Anat Rec*. 1997;247:388–94.

[11] Vischer UM, Wagner DD. CD63 is a component of Weibel–Palade bodies of human endothelial cells. *Blood*. 1993;82:1184–91. https://doi.org/10.1182/blood.V82.4.1184.1184

[12] Schnyder-Candrian S, Borsig L, Moser R, Berger EG. Localization of alpha 1,3-fucosyltransferase VI in Weibel-Palade bodies of human endothelial cells. *Proc Natl Acad Sci U S A*. 2000;97:8369–1191.

[13] Huber D, Cramer EM, Kaufmann JE, Meda P, Masse JM, Kruithof EK, Vischer UM. Tissue-type plasminogen activator (t-PA) is stored in Weibel–Palade bodies in human endothelial cells both in vitro and in vivo. *Blood*. 2002;99:3637–45.

[14] van Breevoort D, van Agtmaal EL, Dragt BS, Gebbinck JK, Dienava-Verdoold I, Kragt A, Bierings R, Horrevoets AJ, Valentijn KM, Eikenboom JC, Fernandez-Borja M, Meijer AB, Voorberg J. Proteomic screen identifies IGFBP7 as a novel component of endothelial cell-specific Weibel–Palade bodies. *J Proteome Res*. 2012;11:2925–36.

[15] Bierings R, van den Biggelaar M, Kragt A, Mertens K, Voorberg J, van Mourik JA. Efficiency of von Willebrand factor-mediated targeting of interleukin-8 into Weibel-Palade bodies. *J Thromb Haemost*. 2007;5:2512–9.

[16] Shahbazi S, Lenting PJ, Fribourg C, Terraube V, Denis CV, Christophe OD. Characterization of the interaction between von Willebrand factor and osteoprotegerin. *J Thromb Haemost*. 2007;5:1956–62.

[17] Babich V, Knipe L, Hewlett L, Meli A, Dempster J, Hannah MJ, Carter T. Differential effect of extracellular acidosis on the release and dispersal of soluble and membrane proteins secreted from the Weibel-Palade body. *J Biol Chem*. 2009;284:12459–68.

[18] Starke RD, Ferraro F, Paschalaki KE, Dryden NH, McKinnon TA, Sutton RE, Payne EM, Haskard DO, Hughes AD, Cutler DF, Laffan MA, Randi AM. Endothelial von Willebrand factor regulates angiogenesis. *Blood*. 2011;117:1071–80.

[19] Randi AM, Smith KE, Castaman G. von Willebrand factor regulation of blood vessel formation. *Blood*. 2018;132:132–40.

[20] Xu H, Cao Y, Yang X, Cai P, Kang L, Zhu X, Luo H, Lu L, Wei L, Bai X, Zhu Y, Zhao BQ, Fan W. ADAMTS13 controls vascular remodeling by modifying VWF reactivity during stroke recovery. *Blood*. 2017;130:11–22.

[21] Maisonpierre PC, Suri C, Jones PF, Bartunkova S, Wiegand SJ, Radziejewski C, Compton D, McClain J, Aldrich TH, Papadopoulos N, Daly TJ, Davis S, Sato TN, Yancopoulos GD. Angiopoietin-2, a natural antagonist for Tie2 that disrupts in vivo angiogenesis. *Science*. 1997;277:55–60.

[22] Imhof BA, Aurrand-Lions M. Angiogenesis and inflammation face off. *Nat Med*. 2006;12:171–2.

[23] Yuan HT, Khankin EV, Karumanchi SA, Parikh SM. Angiopoietin 2 is a partial agonist/antagonist of Tie2 signaling in the endothelium. *Mol Cell Biol*. 2009;29:2011–22.

[24] McKinnon TA, Chion AC, Millington AJ, Lane DA, Laffan MA. N-linked glycosylation of VWF modulates its interaction with ADAMTS13. *Blood*. 2008;111:3042–9.

[25] Nowak AA, Canis K, Riddell A, Laffan MA, McKinnon TA. O-linked glycosylation of von Willebrand factor modulates the interaction with platelet receptor glycoprotein Ib under static and shear stress conditions. *Blood*. 2012;120:214–22.

[26] Flood VH, Gill JC, Morateck PA, Christopherson PA, Friedman KD, Haberichter SL, Branchford BR, Hoffmann RG, Abshire TC, Di Paola JA, Hoots WK, Leissinger C, Lusher JM, Ragni MV, Shapiro AD, Montgomery RR. Common VWF exon 28 polymorphisms in African Americans affecting the VWF activity assay by ristocetin cofactor. *Blood*. 2010;116:280–6.

[27] Kim I, Kim JH, Ryu YS, Liu M, Koh GY. Tumor necrosis factor-alpha upregulates angiopoietin-2 in human umbilical vein endothelial cells. *Biochem Biophys Res Commun*. 2000;269:361–5.

[28] van den Biggelaar M, Bouwens EA, Kootstra NA, Hebbel RP, Voorberg J, Mertens K. Storage and regulated secretion of factor VIII in blood outgrowth endothelial cells. *Haematologica*. 2009;94:670–8.

[29] Ramsay DM, Buist TA, Macleod DA, Heading RC. Persistent gastrointestinal bleeding due to angiodysplasia of the gut in von Willebrand's disease. *Lancet*. 1976;2:275–8.

[30] Franchini M, Mannucci PM. Gastrointestinal angiodysplasia and bleeding in von Willebrand disease. *Thromb Haemost*. 2014;112:427–31.

[31] Makris M. Gastrointestinal bleeding in von Willebrand disease. *Thromb Res*. 2006;118(Suppl 1):S13–7.

[32] Starke RD, Paschalaki KE, Dyer CE, Harrison-Lavoie KJ, Cutler JA, McKinnon TA, Millar CM, Cutler DF, Laffan MA, Randi AM. Cellular and molecular basis of von Willebrand disease: studies on blood outgrowth endothelial cells. *Blood*. 2013;121:2773–84.

[33] Selvam SN, Casey LJ, Bowman ML, Hawke LG, Longmore AJ, Mewburn J, Ormiston ML, Archer SL, Maurice DH, James P. Abnormal angiogenesis in blood outgrowth endothelial cells derived from von Willebrand disease patients. *Blood Coagul Fibrinolysis*. 2017;28:521–33.

[34] Llopis J, McCaffery JM, Miyawaki A, Farquhar MG, Tsien RY. Measurement of cytosolic, mitochondrial, and Golgi pH in single living cells with green fluorescent proteins. *Proc Natl Acad Sci U S A*. 1998;95:6803–8.

[35] Chanat E, Huttner WB. Milieu-induced, selective aggregation of regulated secretory proteins in the trans-Golgi network. *J Cell Biol*. 1991;115:1505–19.

[36] Wu MM, Grabe M, Adams S, Tsien RY, Moore HP, Machen TE. Mechanisms of pH regulation in the regulated secretory pathway. *J Biol Chem*. 2001;276:33027–35.

[37] Ishihara J, Ishihara A, Starke RD, Peghaire CR, Smith KE, McKinnon TAJ, Tabata Y, Sasaki K, White MJV, Fukunaga K, Laffan MA, Lutolf MP, Randi AM, Hubbell JA. The heparin binding domain of von Willebrand factor binds to growth factors and promotes angiogenesis in wound healing. *Blood*. 2019;133:2559–69.

[38] Rastegar-Lari G, Villoutreix BO, Ribba AS, Legendre P, Meyer D, Baruch D. Two clusters of charged residues located in the electropositive face of the von Willebrand factor A1 domain are essential for heparin binding. *Biochemistry*. 2002;41:6668–78.

[39] Groeneveld DJ, Sanders YV, Adelmeijer J, Mauser-Bunschoten EP, van der Bom JG, Cnossen MH, Fijnvandraat K, Laros-van Gorkom BAP, Meijer K, Lisman T, Eikenboom J, Leebeek FWG. Circulating angiogenic mediators in patients with moderate and severe von Willebrand disease: a multicentre cross-sectional study. *Thromb Haemost*. 2018;118:152–60.

[40] van den Biggelaar M, Bouwens EA, Voorberg J, Mertens K. Storage of factor VIII variants with impaired von Willebrand factor binding in Weibel-Palade bodies in endothelial cells. *PLOS One*. 2011;6:e24163.

[41] Pipe SW, Montgomery RR, Pratt KP, Lenting PJ, Lillicrap D. Life in the shadow of a dominant partner: the FVIII–VWF association and its clinical implications for hemophilia A. *Blood*. 2016;128:2007–16.

[42] Orfanos SE, Kotanidou A, Glynos C, Athanasiou C, Tsigkos S, Dimopoulou I, Sotiropoulou C, Zakynthinos S, Armaganidis A, Papapetropoulos A, Roussos C. Angiopoietin-2 is increased in severe sepsis: correlation with inflammatory mediators. *Crit Care Med*. 2007;35:199–206.

[43] Siner JM, Bhandari V, Engle KM, Elias JA, Siegel MD. Elevated serum angiopoietin 2 levels are associated with increased mortality in sepsis. *Shock*. 2009;31:348–53.

[44] Parikh SM, Mammoto T, Schultz A, Yuan HT, Christiani D, Karumanchi SA, Sukhatme VP. Excess circulating angiopoietin-2 may contribute to pulmonary vascular leak in sepsis in humans. *PLoS Med*. 2006;3:e46.

[45] Mobayen G, Dhutia A, Clarke C, Prendecki M, McAdoo S, Keniyopoullos R, Malik T, Laffan M, Willicombe M, McKinnon T. Severe COVID-19 is associated with endothelial activation and abnormal glycosylation of von Willebrand factor in patients undergoing hemodialysis. *Res Pract Thromb Haemost*. 2021;5:e12582.

[46] Philippe A, Chocron R, Gendron N, Bory O, Beauvais A, Peron N, Khider L, Guerin CL, Goudot G, Levasseur F, Peronino C, Duchemin J, Brichet J, Sourdeau E, Desvard F, Bertil S, Pene F, Cheurfa C, Szwebel TA, Planquette B, et al. Circulating von Willebrand factor and high molecular weight multimers as markers of endothelial injury predict COVID-19 in-hospital mortality. *Angiogenesis*. 2021;24:505–17.

[47] Wohner N, Sebastian S, Muczynski V, Huskens D, de Laat B, de Groot PG, Lenting PJ. Osteoprotegerin modulates platelet adhesion to von Willebrand factor during release from endothelial cells. *J Thromb Haemost*. 2022;20:755–66.